

GALACTIC HALO CUSP/CORE: STEEPENING BY TIDAL COMPRESSION

Avishai Dekel & Jonathan Devor

Racah Institute of Physics, The Hebrew University, Jerusalem 91904, Israel

ABSTRACT

We explain in simple terms how the buildup of dark halos by merging satellites inevitably leads to an inner cusp of density profile $\rho \propto r^{-\alpha}$ with $\alpha \gtrsim 1$, as seen in cosmological N-body simulations. A flatter core with $\alpha < 1$ exerts on each satellite tidal compression in all directions, which prevents deposit of stripped satellite material in this region. This makes the satellite orbits decay from the radius where $\alpha \sim 1$ to the halo center with no tidal mass transfer in the core and thus causes a rapid steepening of the inner profile. The transition at $\alpha \sim 1$ is addressed qualitatively in the extreme limits of impulse and adiabatic approximations and using tidal radii for satellites on radial and circular orbits. These tidal effects and the resulting steepening of the profile are then demonstrated using merger N-body simulations. In an associated paper we address the subsequent slow convergence to an asymptotic stable cusp with $\alpha \gtrsim 1$. Our result implies that an inner cusp is enforced as long as enough satellite material makes it intact into the inner halo and is deposited there. We conclude that in order to maintain a flat core as indicated by observations, CDM satellites must be disrupted outside the core. This could be the result of puffing up of small halos due to baryonic feedback processes, which could actually be stimulated by the same effect of tidal compression in the halo core.

1. INTRODUCTION

Cosmological N-body simulations of dissipationless hierarchical clustering from Gaussian initial fluctuations reveal a relatively robust universal shape for the density profile of dark-matter halos,

$$\rho(r) = \rho_s \left(\frac{r}{r_s} \right)^{-\alpha_0} \left(1 + \frac{r}{r_s} \right)^{\alpha_0-3}, \quad (1)$$

where r_s is a characteristic inner radius and ρ_s a corresponding inner density. It has an inner “cusp” $\propto r^{-\alpha_0}$, a turn-over near r_s , and an outer envelope of r^{-3} extending out to

the virial radius R_v (defined by a fixed mean overdensity Δ_v above the universal mean, with $\Delta_v = 180$ to 340 , depending on time and the cosmological model). Navarro, Frenk & White (1995; 1996; 1997, hereafter NFW) found eq. (1) with $\alpha_0 \simeq 1$ to be a good fit to halos in simulations over the radius range $(0.01 - 1)R_v$, for a wide range of halo masses and for a range of hierarchical cosmological scenarios with different power spectra of initial fluctuations. Cole & Lacey (1996) came to a similar conclusion for self-similar scenarios with power-law power spectra, $P_k \propto k^n$ with $n = 0, -1, -2$, in an Einstein-deSitter cosmology. High-resolution simulations of a few individual halos in a cosmological environment (Moore *et al.* 1998; Ghigna *et al.* 2000; Klypin *et al.* 2001) found that the typical asymptotic cusp profile at $r \ll r_s$ is sometimes somewhat steeper, closer to $\alpha_0 \simeq 1.5$. A careful convergence analysis by Power *et al.* (2002), who explored the robustness to numerical errors, found for the standard Λ CDM cosmology that α_0 reaches a slope shallower than 1.2 at their innermost resolved point of $r \sim 0.005R_v$. While the formation of a cusp with a characteristic slope $1 \leq \alpha_0 \leq 1.5$ has been established in the simulations, a basic theoretical understanding of its origin is still lacking.

An even more intriguing puzzle is introduced by observations of low surface-brightness (LSB) galaxies, whose centers are dominated by their dark matter halos, which indicate that at least in some cases their actual inner halo density profiles are close to flat cores, with $\alpha_0 \simeq 0$ (van den Bosch *et al.* 2000; de Block *et al.* 2001). Similar cores may be present in other galaxies (Salucci & Burkert 2000; Salucci 2001; Borriello & Salucci 2001). This seems to introduce a severe challenge to the CDM cosmological paradigm. Attempts to turn a cusp into a core by direct stellar feedback effects in the present halos, which looked promising at a first sight (Navarro, Eke & Frenk 1996) seem not to work (e.g., Geyer & Burkert 2001; Gnedin & Zhao 2002).

In order to make progress in resolving the core problem, we find it useful to first try to understand in simple basic terms the origin of the universal cusp in the gravitational N-body simulations of cold dark matter. This should provide us with a tool for addressing the formation of flat cores by other mechanisms, in particular by baryonic feedback processes within the hierarchical CDM framework.

Back to the issue of dark-halo profiles in dissipationless simulations, the outer slope of r^{-3} (and steeper) may possibly be explained in terms of violent relaxation (e.g., Barnes & Hernquist 1991; Pearce, Thomas & Couchman 1993 and references therein). In general, any finite system would tend to have a steep density fall off at large radii due to diffusion of particles outwards. Secondary spherical infall is expected to produce a profile closer to $\rho \propto r^{-2}$, which may explain the behavior in the intermediate regions of the halo, but is too steep to explain the flatter inner cusp (Lokas & Hoffman 2000 and references therein). Thus,

none of the above mechanisms provides a natural explanation for the characteristic cusp of $\alpha \gtrsim 1$.

By watching the evolution in cosmological N-body simulations of hierarchical clustering scenarios, we know that halos are largely built up by a sequence of mergers of smaller halos. In a typical merger, a bound satellite halo spirals into the center of the larger halo due to gravity and dynamical friction. The satellite gradually transfers mass into the host halo due to tidal stripping or by eventually melting into the halo inner region. This process is likely to have an important effect in shaping up the density profile. Indeed, Syer & White (1998) and Nusser & Sheth (1999) argued, using certain simple models and simulations of a sequence of mergers, that the buildup by mergers may naturally lead to a stable profile. However, they find their predicted profile to be quite sensitive to the power spectrum of fluctuations and to allow an inner slope of $\alpha < 1$, in conflict with the robust result of the cosmological simulations. In fact, when trying to repeat the Syer & White analysis using their simplified modeling of the stripping process but with higher resolution, we find that in the long run the profile does not really converge to a stable cusp but rather continues to steepen slowly towards $\alpha_0 = 3$. Either way, it seems that something is not adequate in the simplified model adopted to describe the mass transfer from the satellite to the halo.

We re-visit the buildup of halo profile by merging satellites and gain an encouraging new insight. We add two important new ingredients to the tidal effects. In the current paper, we argue that for a flat mean density profile with $\alpha \leq 1$ the tidal effects on typical satellites induce three-dimensional compression with no local mass deposit, which results in a rapid steepening of the inner profile to $\alpha > 1$. In an associated paper (Dekel *et al.* 2002) we derive a useful prescription for tidal mass transfer at $\alpha > 1$, and obtain higher deposit efficiency at higher α . We then show that this tends to flatten steep profiles with large α and thus slowly leads to an asymptotic fixed point at a certain $\alpha = \alpha_a \gtrsim 1$.

In §2 we address the α dependence of the tidal force and highlight the three-dimensional tidal compression in a core of $\alpha < 1$. In §3 we qualitatively evaluate the transition in mass-transfer efficiency at $\alpha \sim 1$ in the extreme limits of impulse and adiabatic tidal effects along typical satellite orbits. In §4 we continue to study the α dependence of the mass transfer using the tidal radii for mergers on radial and circular orbits. In §5 we describe N-body merger simulations and use them for testing the predictions of our simple model. In §7 we summarize the analysis leading to an asymptotic cusp $\alpha \rightarrow \alpha_a > 1$. In §8 we speculate about a possible scenario for maintaining a flat core based on tidal compression and baryonic feedback. In §9 we discuss our results.

2. TIDAL FORCE: COMPRESSION AND STRETCHING

We consider a spherical halo of mass profile $M(r)$ and virial mass M_v . The *mean* density in a sphere of radius r is $\bar{\rho}(r) \propto M(r)/r^3$. A useful quantity in describing the tidal forces exerted by this halo is its local logarithmic slope,

$$\alpha(r) \equiv -\frac{d \ln \bar{\rho}}{d \ln r}, \quad (2)$$

such that locally $\bar{\rho} \propto r^{-\alpha}$. We assume that α is either constant or monotonically increasing as a function of r , with values in the range $0 \leq \alpha \leq 3$. The extreme values of $\alpha = 0$ and 3 correspond to a constant-density halo and a point mass respectively. Note that if the profile inside r is a power law, then the local and mean density profiles have the same logarithmic slope. In general, they are related via $\rho(r) = [1 - \alpha(r)/3]\bar{\rho}(r)$, but they do not necessarily have the same slope at a given r . The slope of $\rho(r)$ is equal to or larger than the slope of $\bar{\rho}(r)$. The following analysis refers to α as the slope of $\bar{\rho}(r)$.

In the analytic part of our analysis we assume that the density profile of the original halo mass is fixed in time throughout the merger while the mass torn from the satellite is gradually being added to the halo. This is confirmed to be a reasonable approximation in our N-body merger simulations, where the mass ratio is 1:10 (e.g. Fig. 3).

We then consider a satellite of mass $m_v \ll M_v$, moving under the gravity exerted by the halo, when its center of mass is at position \mathbf{r} as measured from the halo center. The tidal acceleration exerted by the halo mass distribution on a satellite particle at position vector $\boldsymbol{\ell}$ relative to the satellite center of mass is obtained by transforming the gravitational attraction exerted by the halo on the particle into the (non-rotating)¹ rest frame of the satellite, namely, by subtracting the acceleration of the satellite center of mass relative to the halo,

$$\mathbf{F}_t = -\frac{GM(|\mathbf{r} + \boldsymbol{\ell}|)(\mathbf{r} + \boldsymbol{\ell})}{|\mathbf{r} + \boldsymbol{\ell}|^3} + \frac{GM(r)\mathbf{r}}{r^3}. \quad (3)$$

In the tidal limit $\ell \ll r$, this yields to first order in ℓ/r

$$\mathbf{F}_t = \frac{G\ell}{r^3} \left([3M(r) - M'(r)r] (\hat{\mathbf{r}} \cdot \hat{\boldsymbol{\ell}}) \hat{\mathbf{r}} - M(r) \hat{\boldsymbol{\ell}} \right), \quad (4)$$

where $M'(r) \equiv dM/dr$. This expression can be simplified using the definition of $\alpha(r)$, which gives $M'(r)r = [3 - \alpha(r)]M(r)$. Using Cartesian coordinates about the satellite center, where $\boldsymbol{\ell} = (\ell_1, \ell_2, \ell_3)$ and $\boldsymbol{\ell}_1$ lies along \mathbf{r} , we get

$$\mathbf{F}_t = \frac{GM(r)}{r^3} ([\alpha(r) - 1]\boldsymbol{\ell}_1 - \boldsymbol{\ell}_2 - \boldsymbol{\ell}_3). \quad (5)$$

¹in some cases it is useful to perform the analysis in a rotating frame, see §4

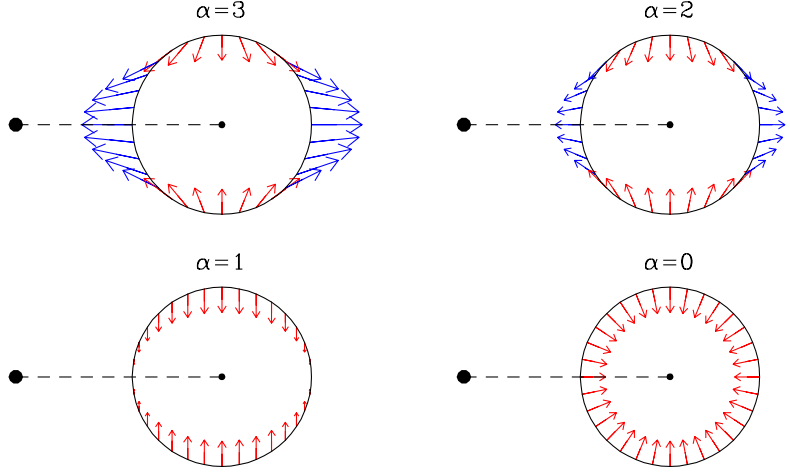


Fig. 1.— Tidal acceleration at a given satellite shell $\ell \ll r$, for a given $\bar{\rho}(r)$ and for different values of halo slope α [eq. (5) or eq. (6)]. The halo center is to the left: the horizontal dashed line is connecting the centers of mass (\mathbf{r}) and the angle θ is measured from this line. At $\cos \theta = 0$ there is always compression, independent of α . Along the line $\cos \theta = \pm 1$ there is stretching for $\alpha > 1$ and compression for $\alpha < 1$.

Alternatively, moving to polar coordinates, where θ is the angle between ℓ and \mathbf{r} and $\hat{\mathbf{r}} = \cos \theta \hat{\ell} - \sin \theta \hat{\theta}$, we obtain

$$\mathbf{F}_t = \frac{GM(r)\ell}{r^3} \left([\alpha(r) \cos^2 \theta - 1] \hat{\ell} - \alpha(r) \sin \theta \cos \theta \hat{\theta} \right). \quad (6)$$

Fig. 1 illustrates the tidal acceleration at a given satellite shell of radius ℓ in a plane that includes the position vector \mathbf{r} connecting the centers of mass, for given r and $M(r)$ and for different slopes $\alpha = 3, 2, 1$ and 0 . The tidal components along ℓ_2 and ℓ_3 , perpendicular to \mathbf{r} , are always negative, namely, they exert compression, and they do not explicitly depend on α . Stretching outwards may occur only along $\pm \mathbf{r}$. Unlike the common notion of tidal forces as pulling outwards, the average force on a sphere of radius ℓ is actually inwards: $\langle \mathbf{F}_t \rangle = (GM/r^3)(\alpha/3 - 1)\ell$. It vanishes for a point-mass perturber, $\alpha = 3$, and it obtains a maximum amplitude in a core where $\alpha = 0$.

The maximum radial tidal force outwards (towards $+\hat{\ell}$) is obtained along $\pm \mathbf{r}$. In the limit where the tides are exerted by a point-mass halo, $\alpha = 3$, the pull outwards is maximal. For flatter halo slopes, the tidal stretching becomes weaker in proportion to $(\alpha - 1)$, until it vanishes at $\alpha = 1$ and reverses direction into compression for $\alpha < 1$. This direction reversal of the tides is often overlooked, because the common context of tides is a perturbation by a concentrated mass distribution. It is a simple result of the fact that the amplitude of the gravitational attraction by the halo, $GM(r)/r^2$, is not a decreasing function of r where the

halo mass profile is rising rapidly enough (faster than $M \propto r^2$). Thus, while for $\alpha > 1$ there is always a tidal component pulling outwards, for $\alpha < 1$ the tidal forces are of compression for any θ , namely everywhere in the satellite. In the limit of a constant-density core, $\alpha = 0$, the tides induce symmetric compression in all three dimensions.

We note that the critical slope of unity is the asymptotic inner slope of the cusp in the NFW profile. We argue that this is not a coincidence. The key idea is that if the local tidal mass transfer from the satellite to the halo stops when the satellite’s orbit has decayed into a core region where $\alpha(r) \leq 1$, the satellite would continue to sink in due to dynamical friction without mass loss until it settles in the halo center. This would inevitably cause a general steepening of the core profile towards $\alpha > 1$. For this scenario to be valid one should verify that, indeed, there is no tidal transfer of mass from the satellite to the halo in a region where $\alpha \leq 1$. We address this point in simple cases using crude analytic approximations and then demonstrate the anticipated effects using N-body simulations.

3. THE IMPULSE AND ADIABATIC LIMITS

The α dependence of the tidal stripping process in the central regions of a halo can be qualitatively evaluated in two extreme limits. If the tidal forces vary on a time scale shorter than the particle orbital periods within the satellite, then one can use the impulse approximation (Spitzer 1958; Binney & Tremaine 1987, hereafter BT, §7.2) to estimate the energy input into the satellite and the resulting mass loss. If the tidal forces vary on a time scale longer than the orbital periods within the satellite, then one can appeal to adiabatic invariants along the particle orbits (e.g., BT §3.7) in order to estimate the gradual energy change of the satellite particles, the associated structural changes in the satellite, and the escape rate.

3.1. Orbits, Stripping and Deposit

The validity of each approximation depends on the nature of the orbit of the satellite within the halo. Along a typical orbit, the satellite distance from the halo center oscillates periodically between the radii of apocenter r_a and pericenter r_p , while their amplitudes gradually decay due to dynamical friction. Ghigna *et al.* (1998) studied the distribution of satellite orbits in a high-resolution N-body simulation of a cluster emerging from a CDM cosmological background (mostly in an extended range where $\alpha \sim 2$). They found that the median ratio r_a/r_p is 6:1, with about 25% of the orbits more eccentric than 10:1, and con-

cluded that radial orbits are common while circular orbits are rare. The expected more rapid tidal disruption of satellites on radial orbits may indicate that the actual initial distribution of orbits tended/fro even more towards radial orbits.

Ghigna *et al.* (1998) also demonstrated that the tidal radii of the satellites, ℓ_t , are consistent with being determined near pericenter, under the general resonance condition $\bar{\rho}(r_p) \sim \bar{\sigma}(\ell_t)$, where $\bar{\sigma}(\ell) \propto m(\ell)/\ell^3$ is the mean density profile of the satellite. Particles that escape from the satellite can be assumed, on average, to continue on an orbit about the halo center with apocenter and pericenter radii “frozen” at their values near the time of escape, suffering no further decay due to dynamical friction. Since a particle spends most of its time near the apocenter of its orbit, we can vaguely say that the escapers are effectively “deposited” in the halo near the apocenter radius valid at the time of escape.

Very eccentric orbits may involve “penetrating” encounters near pericenter, where $r_p < \ell$ for ℓ a characteristic radius of the satellite. In this case the tidal approximation becomes invalid. The tides are weakened when the center of the perturber lies inside the satellite, until they vanish when the satellite center coincides with the halo center. It can be shown that the effect of a fast penetrating encounter is comparable to the effect of an encounter with $r_p \sim \ell$ as computed using the impulse approximation in the tidal limit (BT §7.2.e). In a slow penetrating situation the tidal effects simply weaken gradually as $r \rightarrow 0$.

3.2. The Impulse Limit

The impulse approximation may be partly valid for satellites on elongated orbits during their first quick pericenter passages. As long as $\alpha > 1$ along the orbit, the tidal force, $F_t \propto \bar{\rho}(r)$, has a peaked maximum at the $\sim r_p$ vicinity of the pericenter, where the satellite spends a small fraction of its orbital period. Since $\bar{\rho}(r_p) \sim \bar{\sigma}(\ell_t)$, and since the typical orbital period is inversely proportional to the square-root of the density, the satellite orbital period is comparable to the internal orbital periods of outer satellite particles. Therefore, the impulse approximation may be partly valid for such particles near their apocenters within the satellite.

In the impulse approximation, each satellite particle is assumed to obtain an instantaneous velocity kick $\Delta\mathbf{v}$, which is the integral $\int \mathbf{F}_t dt$ over the short duration of effective tides near pericenter along the satellite orbit. The energy change per unit mass of a particle moving with momentary velocity \mathbf{v} is thus $\Delta E = (1/2)(\mathbf{v} + \Delta\mathbf{v})^2 - (1/2)\mathbf{v}^2$, which consists of linear and quadratic terms in $\Delta\mathbf{v}$, namely

$$\Delta E = \mathbf{v} \cdot \Delta\mathbf{v} + (1/2)(\Delta\mathbf{v})^2. \quad (7)$$

Some particles may be kicked by this impulse to above the escape velocity at their position and become unbound.

If the satellite is spherical and the particle motions outwards and inwards are symmetric, a kick inwards is as effective in feeding energy into the satellite as a kick outwards. The contribution of the linear term to the total energy vanishes by the symmetry of incoming and outgoing particles, but the linear term may have an important contribution for the escapers which come from the high-end tail of the ΔE distribution.

The dominant tidal kick $\Delta \mathbf{v}$ is inwards, along the direction perpendicular to the orbital plane, where the tidal force is α -independent and persistently inwards. A somewhat smaller kick is induced along the position vector of the satellite (\mathbf{r}) at pericenter (it is a net kick inwards if $\alpha < 2$), while the contribution along the position vector at apocenter tends to average out when integrated along the orbit (BT §7.2, eq. 7-54; Gnedin, Hernquist & Ostriker 1999).

If indeed $\bar{\rho}(r_p) \sim \bar{\sigma}(\ell_t)$, then the velocity kick integrated along a path of length $\sim r_p$ near pericenter is comparable to the typical particle velocity, $\Delta v \sim v \sim \bar{\rho}(r_p)^{1/2} \ell_t$. This makes the energy change maximal in the outer satellite regions, with comparable contributions from the linear and quadratic terms. The kick inwards causes a delayed escape, because the escapers need to cross the satellite before departure, and the crossing time is comparable to the orbital period in the halo. Therefore, the actual stripping is expected to occur in the halo near the following apocenter, where the particle is “deposited” anyway (§3.1).

When apocenter is at $\alpha > 1$ but pericenter is already in the $\alpha < 1$ regime, the duration of maximum tides becomes longer and the impulse approximation less valid. Any stripping that still occurs along such an orbit ends up with “deposit” outside the $\alpha < 1$ core.

Once the satellite orbit becomes confined to the inner halo where $\alpha < 1$, we expect no impulse stripping. If the slope near pericenter is α , the tidal force drops to half its peak magnitude at a distance of $\sim 2^{1/\alpha} r_p$ from pericenter. At $\alpha = 1/2$ this is already $4r_p$, so the tidal force is not much weaker than its pericenter value throughout a large fraction of the orbit. Furthermore, adiabatic compression makes $\bar{\sigma}$ become larger than $\bar{\rho}(r_p)$ (§3.3 below). These two effects make the impulse approximation invalid. The effect of the inwards tidal force accelerating an incoming particle is roughly balanced by the inwards tidal force of similar magnitude working to decelerate the particle when it is going out. In the limit where $\alpha = 0$, the tidal force is the same in all directions and constant in time, so $\int \mathbf{F}_t dt = 0$ along each particle orbit and there is no net impulse.

We conclude that we expect no impulse tidal mass deposit in the core region where $\alpha < 1$: neither during the early quick core passages nor after the decay of the orbit into the

core region.

3.3. The Adiabatic Limit

The adiabatic invariance of actions, which is formally valid when the internal orbital periods are much shorter than the characteristic time over which the external potential is varying, is known to be crudely applicable even when these time scales are comparable to each other (BT, §3.6, Fig. 3-29). Since $\bar{\rho}(r_p) \sim \bar{\sigma}(\ell_t)$, and since for bound satellite particles along the satellite orbit $\ell \leq \ell_t$ and $r \geq r_p$, the satellite particles inwards of the tidal radius are likely to obey the adiabatic approximation at all times. Once the decayed orbit becomes confined to a central halo region of $\alpha < 1$, where the tidal force varies slowly along the orbit and actually tends to a constant when $\alpha \rightarrow 0$, the adiabatic approximation becomes crudely applicable also for the outer satellite particles. Any adiabatic compression of the satellite would strengthen the applicability of this approximation.

In this case, the tides gradually distort the satellite, and may cause slow mass loss mostly outside a momentary tidal radius. Now tidal forces outwards cause stretching and energy gain, which may lead to mass loss, while tidal forces inwards cause contraction, make the satellite more bound and do not lead to stripping.

In order to gain some insight into the α dependence of adiabatic tidal effects we consider the following simple example. We see in eq. (5) that the tidal perturbation in each direction ($i = 1, 3$) mimics the force of a harmonic oscillator about the satellite center,

$$F_{ti} = -k_{ti}\ell_i, \quad k_{ti} \propto \bar{\rho}(r) [(1 - \alpha), 1, 1], \quad (8)$$

except that the force constant along ℓ_1 is negative for $\alpha > 1$. If we assume as a toy model that the satellite core is a homogeneous sphere with density σ_0 , the orbits under its own self gravity are also three-dimensional harmonic oscillators, with

$$F_{0i} = -k_{0i}\ell_i, \quad k_{0i} \propto \sigma_0. \quad (9)$$

This can be generalized to a homogeneous ellipsoid, with different force constants in the different directions, based on Newton's third theorem (e.g. BT, §2.3, Table 2-1). The perturbed system is thus a 3-dimensional harmonic oscillator, with force constants $k_i = k_{0i} + k_{ti}$, and corresponding frequencies $w_i^2 = k_i$. If the motion of the satellite within the halo introduces slow variations in the tidal perturbation, and correspondingly in k_i , the particles should conserve adiabatic invariants along their orbits. The case of a radial satellite orbit within the halo is particularly simple because the principle directions remain stationary. The

adiabatic invariant of the harmonic oscillator along each direction is the action integral

$$\int v_i^2 dt \propto w_i L_i^2 \propto -E_i/w_i \simeq \text{const.}, \quad (10)$$

where the integral is over the period of the oscillation, L_i is the amplitude of the oscillation, and E_i is the corresponding energy (e.g, BT, §3.6.b). Thus $\Delta E_i \propto -\Delta\omega_i$, meaning that strengthening (weakening) of the force constant k_i , corresponding to an increase (decrease) in w_i , leads to shrinking (stretching) and negative (positive) energy changes. This implies that escape may be caused only for particles moving roughly along the radial-orbit line ($\pm\ell_1$) and only as long as $k_1 \propto \bar{\rho}(r)[1 - \alpha(r)]$ is decreasing while r is decreasing. When the satellite is decaying within a halo core where $\alpha < 1$ and where the forces are towards the satellite center in all directions, all the force constants are clearly increasing with decreasing r , so there is systematic shrinking in all directions. The corresponding energy changes are negative for all the particles, implying no stripping.

When the satellite orbit becomes confined to a flat core of $\alpha = 0$ and density ρ_0 , the restoring force is constant and fully spheri-symmetric, $\mathbf{F} \propto -(\rho_0 + \sigma_0)\ell$, independent of the actual orbit of the satellite within the halo core. The satellite is then in its most tightly bound configuration. We may expect the situation not to be very different for small α values in the range $\alpha < 1$, as the deviation from spherical symmetry is limited to one direction, along which the force is still restoring and is getting stronger as r decreases.

We conclude that the slope of $\alpha \sim 1$ indeed seems to be a critical value below which stripping is not expected to occur.

4. TIDAL RADIUS

The α dependence in a slow stripping process can be studied by means of the momentary tidal radius. This depends on the nature of the orbit of the satellite within the halo, which dictates, for example, whether the most useful frame of reference for defining the tidal radius should be rotating or not.

A lower bound to the tidal radius is obtained rigorously in the (rare) case of a *circular* orbit. If the circular angular velocity is $\boldsymbol{\Omega}$, the potential is stationary in a frame which co-rotates with the same angular velocity, in which the corresponding fictitious centrifugal force should also be taken into account. In this case, the Jacobi integral J is conserved along the orbit of each satellite particle (see BT, §3.3 and §7.3). It is the energy as measured in this rotating frame including in the effective potential the term corresponding to the centrifugal force, $-(\boldsymbol{\Omega} \times \mathbf{x})^2$. The outermost closed zero-velocity surface of constant J defines a firm

closed boundary around the satellite, the Roche lobe, which cannot be crossed by particles from the inside out. Therefore, the distance from the satellite to the Lagrange point, the saddle point of the effective potential, provides a lower bound for the tidal radius. This Lagrange point can be obtained by balancing in the rotating satellite frame the self-gravity of the satellite with the tidal plus centrifugal forces along the line connecting the centers of mass. The self-gravity pull inwards by the satellite mass interior to ℓ is $-[Gm(\ell)/\ell^3]\ell$ and the centrifugal force is of an opposite sign and the same amplitude because of co-rotation [$\Omega^2 \propto M(r)/r^3 = m(\ell)/\ell^3$]. Using the ℓ_1 component of the tidal force from eq. (5) we obtain for the tidal radius when the satellite is on a circular orbit of radius r :

$$\alpha(r) \bar{\rho}(r) = \bar{\sigma}(\ell_t) \quad (11)$$

(compare to BT, eq. 7-84, for the case $\alpha = 3$). In this case the combined effect of the tidal and centrifugal forces along the line connecting the centers of mass is always pointing away from satellite center, towards $+\hat{\ell}$. This stretching force becomes weaker as α decreases, but it completely vanishes only at $\alpha = 0$. In the direction perpendicular to the line connecting the centers of mass but still in the merger plane the tidal compression along $-\hat{\ell}$ is exactly balanced by the centrifugal force, independent of r and α . In the direction perpendicular to the merger plane, the centrifugal force is zero so the net force is the usual tidal compression, with no explicit α dependence.

In the other extreme (more realistic) case of a merger on a *radial* orbit, the only forces working on the particle in the satellite (non-rotating) rest frame are the tidal force and the self-gravity pull inwards. The direction of maximum tides is stationary, and only the magnitude of the force varies as a function of r . Even though there is no exact analog of the Jacoby integral in this case, one may still define a tidal radius ℓ_t by the point along the line of maximum tides at which the tidal and self-gravity forces balance each other such that the net force in the satellite frame is zero. The condition replacing eq. (11) for a radial orbit is thus

$$[\alpha(r) - 1] \bar{\rho}(r) = \bar{\sigma}(\ell_t). \quad (12)$$

In the above expressions for the tidal radius, the satellite profile is crudely assumed to be fixed in time for $\ell < \ell_t$ and its mass distribution is assumed to remain spherical; the shells outside the tidal radius are assumed to be peeled like layers off an onion while the tidal distortions are neglected.

We now investigate the evolution of the tidal radius, starting with the radial-orbit case. As r is decreasing from the virial radius inwards, where α is large, the function $[\alpha(r) - 1] \bar{\rho}(r)$ is increasing. Assuming that $\bar{\sigma}(\ell)$ is a monotonically decreasing function, this means that ℓ_t is decreasing. More and more mass of the satellite is being torn away as the satellites

is moving in. However, as the satellite approaches the position where α approaches unity, the function $[\alpha(r) - 1] \bar{\rho}(r)$ approaches zero, implying that the tidal radius grows to infinity. This means that there is a halo radius r_m and a corresponding slope $\alpha_m > 1$ at which $[\alpha(r) - 1] \bar{\rho}(r)$ obtains a maximum. If the inner satellite density is high enough then eq. (12) implies that $\bar{\sigma}(\ell_t)$ obtains a maximum value $\bar{\sigma}_m$ at r_m , and therefore ℓ_t obtains a minimum value ℓ_{tm} there. Since at $r < r_m$ (and $\alpha < \alpha_m$) the tidal radius derived by eq. (12) is larger than ℓ_{tm} , we expect no further stripping inwards of r_m . The slope α_m thus characterizes the point of minimum tidal radius inside which the stripping stops, and ℓ_{tm} marks the central part of the satellite which remains intact, not to be disrupted.

The subsequent sinking in of this whole remnant to the halo center due to dynamical friction causes a steepening of the profile at $r < r_m$ where $\alpha < \alpha_m$. This steepening is effective at least as long as the inner slope is flatter than $\alpha = 1$. It can be avoided only if the inner satellite density is low enough such that $\ell_t = 0$ already at $r > r_m$, namely the satellite is fully disrupted outside the halo core region (see Fig. 7 and §8).

As an example, assume that the *mean* halo density profile is given by eq. (1) with $\rho_s = r_s = 1$, namely $\bar{\rho}(r) = r^{-\alpha_0}(1+r)^{\alpha_0-3}$, and allow the inner slope α_0 to take a value between 0 and 3.² The corresponding α profile is $\alpha(r) = (\alpha_0 + 3r)/(1+r)$ and we find that $[\alpha(r) - 1] \bar{\rho}(r)$ obtains a maximum at $r_m = (1 - \alpha_0)/2 + (3\alpha_0^2 - 12\alpha_0 + 9)^{1/2}/6$. Fig. 2 shows, for a range of α_0 values, the corresponding values of the minimum-tidal-radius quantities r_m , α_m , and the corresponding $\bar{\sigma}(\ell_t)$ according to eq. (12). We see that for a flat core, $\alpha_0 = 0$, the minimum tidal radius is obtained at $\alpha_m = 1.5$ and $r_m = 1$. For larger α_0 in the range $(0, 1)$, the value of α_m gradually decreases towards $\alpha_m = 1$, namely it converges to the asymptotic value $\alpha_0 = 1$ at $r \rightarrow 0$. For $\alpha_0 \geq 1$, the minimum tidal radius is obtained at $r_m = 0$, with $\alpha_m = \alpha_0$. For α_0 in this range the stripping continues until the tidal radius shrinks to zero and the whole satellite is disrupted.

The overall tidal compression at $\alpha < 1$ should actually enhance the steepening effect. It makes the satellite more compact while in the halo core, and effectively adds halo mass to it, which makes the dynamical friction more effective and speeds up the orbit decay to the halo center. Moreover, the halo reacts to the addition of satellite mass to its center by further contraction, preferentially at smaller radii, roughly obeying the adiabatic invariant that requires $Mr \sim \text{const.}$ inside each shell of material.

In the case of a circular orbit, eq. (11), an analogous analysis to the one summarized in Fig. 2, for the example of a mean halo profile given by eq. (1), yields for a core of $\alpha_0 = 0$ a minimum tidal radius at $\alpha_m = 3/4$ (the analog of $\alpha_m = 1.5$ in the radial case). The minimum

²The corresponding local density profile is a Hernquist profile, $\rho(r) = (1 - \alpha_0/3)r^{-\alpha_0}(1+r)^{\alpha_0-4}$.

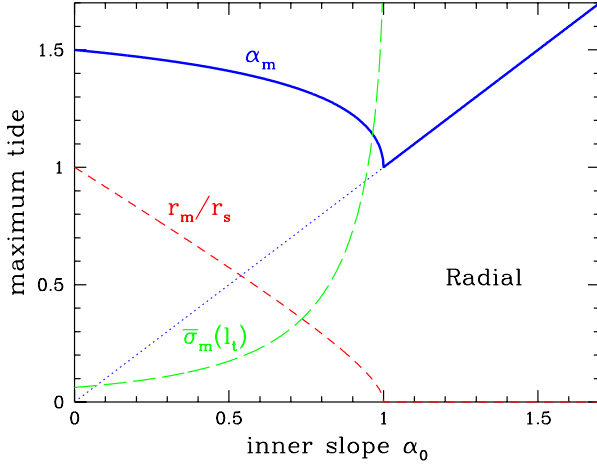


Fig. 2.— Quantities when the tidal radius obtains a minimum, as a function of the halo inner slope α_0 in eq. (1). Shown are the position in the halo r_m/r_s , the slope α_m and the mean density within the minimum tidal radius $\bar{\sigma}_m(l_t)$. Note that $\alpha_m \geq 1$.

tidal radius becomes zero and $\alpha_m = \alpha_0$ for any $\alpha_0 > 3/13$ (the analog of $\alpha_0 > 1$ in the radial case). Since eq. (11) provides a lower bound to the tidal radius, these values of α_m should be regarded as lower bounds.

Since at a given position in a given halo central region (given α) the stripping seems to be more efficient for satellites on circular orbits than on radial orbits, and the compression is correspondingly less effective, the dynamical friction becomes weaker for circular orbits. This should slow down the dynamical-friction decay of the orbit to the halo center and the steepening process.

Thus, based on the current simplified analysis, the satellites on circular orbits are not necessarily as effective as those on radial orbits in steepening cores to cusps. However, we argue in Dekel *et al.* (2002) (and summarize in §7 below) that the α dependence of the mass-transfer efficiency is enough to cause steepening of the profile even by satellites on circular orbits, as is demonstrated by simulations below (§6).

The tidal radius of a satellite on a realistic, elongated orbit is likely to lie in between the radii obeying eq. (12) and eq. (11). At large r (compared to pericenter), an elongated orbit can be approximated as a radial orbit. Near pericenter of an orbit about a point-mass halo the orbit might have resembled a circular orbit, but in a flat halo core the orbit near pericenter is better approximated by a straight line. Thus, the steepening effects of typical satellites on the inner halo profile are more likely to be similar to the effects evaluated for radial orbits.

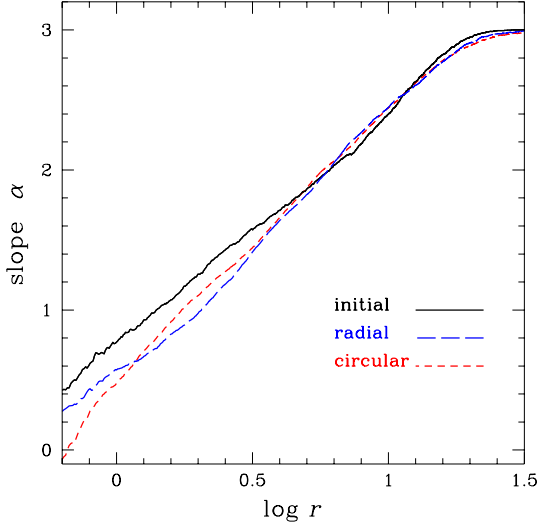


Fig. 3.— The halo profile in the simulation represented by the logarithmic slope α of the mean density profile as a function of radius r (in units of 3.5kpc). Shown are the halo profile at the initial time (solid) and the profiles of the original halo mass at the final times of the radial (long dash) and circular (short dash) merger simulations.

5. MERGER SIMULATIONS

5.1. The Simulations

In order to test the validity of our simple theoretical considerations we ran N-body simulations of isolated mergers between a large halo and a satellite halo of mass ratio $m/M = 0.1$. We use the Tree code by Mihos & Hernquist (1996 and references therein) but with dark-matter halos only (no gaseous disks). The large host halo is represented by 10^5 equal-mass particles and the satellite by 10^4 particles. The simulation units are: length 3.5kpc, mass $5.6 \times 10^{10} M_\odot$, and time 13.06Myr. The force softening length is 0.08 units, i.e. 0.28kpc

The initial halo density profile, as measured in the unperturbed initial conditions, is fit by a truncated isothermal sphere with a flat core,

$$\rho(r) = \frac{\rho_s e^{-(r/r_t)^2}}{1 + (r/r_s)^2}, \quad (13)$$

with $\rho_s = 2.89$, $r_s = 2.08$ and $r_t = 9.86$. The internal velocities are constructed to fulfil the isotropic Jeans equation which ensures an equilibrium configuration as discussed in Mihos & Hernquist (1996). When run in isolation, the halo profile has been tested to be very stable for many dynamical times. The initial halo density profile can be seen in Fig. 6 below. Fig. 3 shows the run of logarithmic slope $\alpha(r)$ for the mean density profile of the initial halo. It

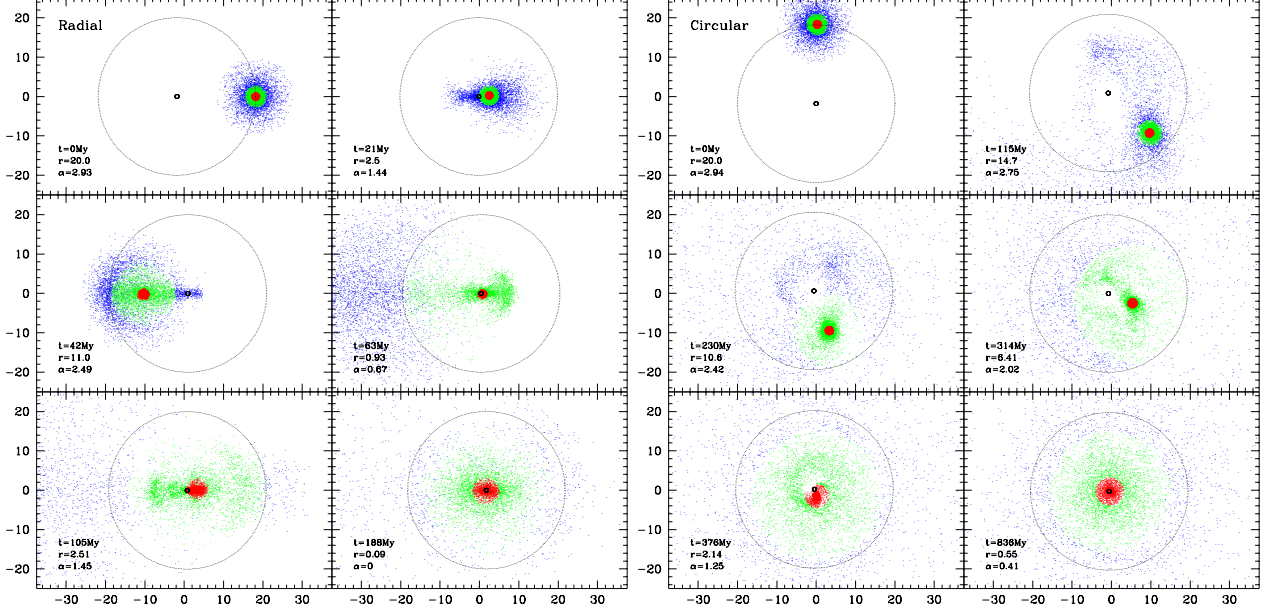


Fig. 4.— The 10^4 satellite particles in 6 snapshots during the radial (left) and circular (right) mergers, projected onto the orbital plane. The 10^5 live halo particles are not shown. The center of mass is at the origin and the dot marks the temporary halo maximum density. The circle is of radius $r = 20 \simeq 2r_t$ about the halo maximum density, corresponding to where the initial halo practically ends and where the satellite is at the onset of the simulation. The three thirds of the mass, in concentric shells about the satellite bound center at each time, are marked by different colors.

spans the range of interest between $\alpha = 0$ and 3, and its variation as a function of radius can be described to a good approximation by $\alpha(r) \approx 1.73 \log r + 0.67$ throughout the range $0.3 \leq \alpha \leq 2.9$. The halo profile resembles the generalized NFW profile of eq. (1) with a core of $\alpha \ll 1$.

The satellite initial density profile is fit by a Hernquist profile,

$$\sigma(\ell) = \frac{\sigma_s}{(\ell/\ell_s) [1 + (\ell/\ell_s)]^3}, \quad (14)$$

with the default choice $\sigma_s = 18.7$ and $\ell_s = 1.0$. The initial satellite density profile can also be seen in Fig. 6. In the inner region it is the NFW profile with $\alpha = 1$.

We simulated three cases of initial merger orbits: a radial orbit, a circular orbit, and an elongated orbit with $r_p/r_a \simeq 1/6$. The unperturbed satellite is put initially at $r = 20$, i.e. at about $2r_t$, where the initial circular period is about 230Myr. In the circular and radial cases the magnitude of the initial satellite velocity was set to equal the circular velocity of

the halo at that radius, namely a bound orbit with an orbital kinetic energy that equals half the absolute value of the total energy. For the elongated orbit the initial tangential velocity was one half of the circular velocity at $r = 20$. Each merger has been followed until the satellite's bound core has practically settled at the halo center.

The radial merger has been followed for more than 200Myr, with equal steps of 1.306Myr between output times. Fig. 4 shows the satellite mass distribution in 6 snapshots during the radial merger process, projected onto one of the orbital planes. The satellite is stretched and stripped along the line connecting the centers of mass and the stripping produces the familiar bridge-and-tail tidal structure. An overall shrinking is seen near the first center crossing, followed by a three-dimensional re-bounce and significant mass loss about the following apocenter, as expected in the impulse limit. The stripped material shows a sequence of arc-like caustic structures corresponding to each apocenter, reflecting the initial confinement in phase space. The oscillations of the satellite remnant about the halo center decay rapidly due to dynamical friction until it becomes confined to the halo core after ~ 115 Myr, and it practically melts into the halo central region after $\sim 130 - 140$ Myr. The final distribution of satellite mass extends quite smoothly about the halo center in a puffy ellipsoid; it is moderately prolate, with the major axis parallel to the original merger line.

The circular merger has been followed for 836Myr with 81 output times spaced by 10.45Myr. Fig. 4 also shows the satellite mass distribution in 6 snapshots during the circular merger process, projected onto the orbital plane. The satellite spirals inwards due to dynamical friction. The gradual tidal stripping process in the outer parts is obvious. Particles escape from the satellite in the two directions roughly along the line connecting the centers of mass of halo and satellite, and produce the familiar trailing and leading tidal tails because of the differential rotation in the halo potential. The remaining bound satellite seems to be slightly elongated in a direction not far from the line connecting the centers of mass, crudely reflecting the shape of the Roche lobe. After entering the halo core, at about 380Myr, the dynamical friction weakens and the satellite orbit continues to decay very slowly towards the halo center. The final distribution of satellite mass extends quite smoothly in a sphere about the halo center.

The behavior in the elongated merger is qualitatively similar to the behavior in the radial merger, so for the sake of saving space we do not display all the figures corresponding to this case.

Fig. 3 also shows the $\alpha(r)$ profiles of the original halo material at the final times after the mergers. The relatively small changes in this profile compared to the changes in the profile of the total halo mass (original halo plus stripped satellite material) indicate that the assumption of a fixed halo to which the satellite mass is being added can serve for a crude

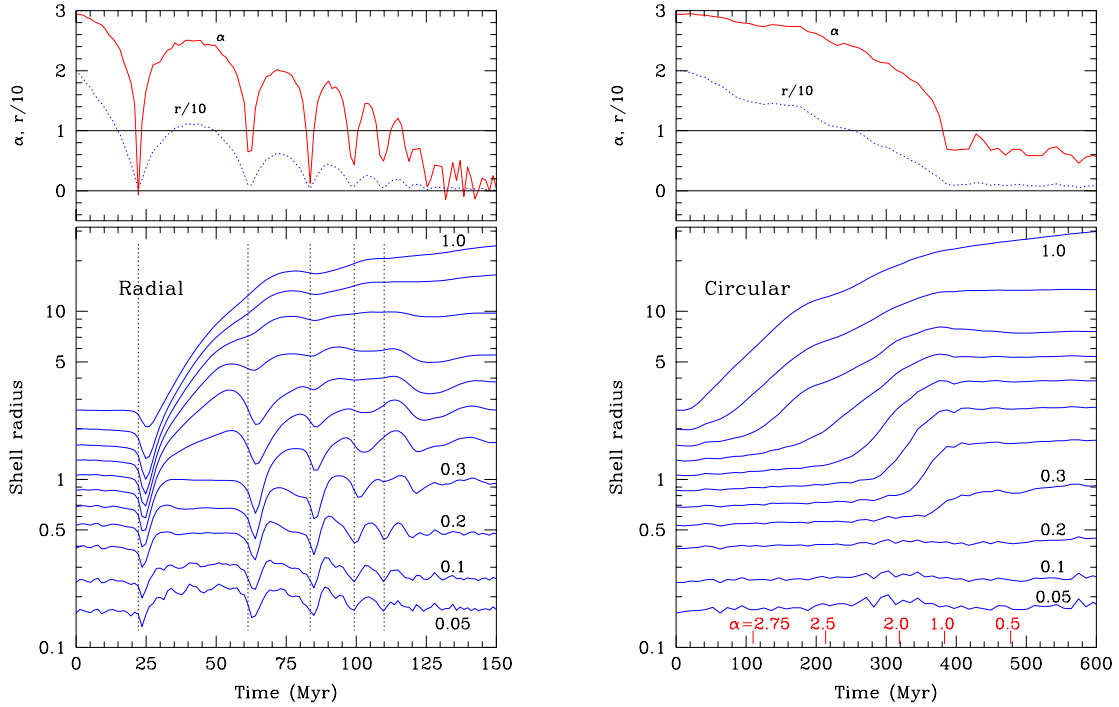


Fig. 5.— Time evolution of the satellite spherical mass profile during the radial merger (left) and the circular merger (right). Shown in the bottom panels are the mean radii of concentric spherical shells about the momentary satellite center, each encompassing a given fraction of the original satellite mass, as labeled on the right. The top panels show the time evolution of position r of the satellite center relative to the halo center (dotted), and the corresponding local slope $\alpha(r)$ (solid). For the radial merger, the times of halo-center crossing are marked in the bottom panel by vertical lines. For the circular merger, representative values of $\alpha(r)$ along the orbit are marked in the bottom panel. The stripping of a shell can be crudely identified by a rapid increase of its radius. Lack of stripping and slight overall contraction of bound shells is noticed whenever the satellite enters the halo core.

toy model.

In all cases the visual impression seems to be consistent with the very crude notion that the particles that are torn away near the pericenter radius are eventually distributed on average about the following apocenter radius, while the bound remnant is gradually sinking into smaller radii due to continuing dynamical friction. This crudely validates the toy-model concept that each satellite shell ℓ is being practically deposited at a certain halo radius r .

6. Testing the Model With the Simulations

Fig. 5 describes the time evolution of the satellite spherical mass profile during the mergers by showing the mean radii of concentric spherical shells about the satellite maximum-density center, each encompassing a given fraction of the satellite mass (i.e., not necessarily the same population of particles at different times).

In the radial merger case the satellite oscillates about $r = 0$. It crosses the halo core back and forth a few times while the oscillation amplitude is decaying due to dynamical friction until the bound remnant settles at the halo center. Center crossings occur at about 22, 62, 83, 99, 110 Myr and so on. The satellite enters the core region in every oscillation a couple of Myr before it crosses the halo center. Indeed, overall contraction of bound satellite shells seems to start roughly at these times, as expected both in the impulse and adiabatic limits. Each major contraction is followed by a re-bounce as the satellite exits the core towards apocenter in the opposite side, which results in overall expansion and stripping of the outer shells. This seems like a manifestation of the expected delayed stripping due to the energy pumped into the satellite by the impulse in the core, and may also reflect adiabatic stretching and stripping outside the tidal radius.

After about 90Myr the satellite orbit becomes confined to inside the region where $\alpha < 1.5$, and after about 107Myr it is confined to the inner halo where $\alpha < 1$. Once the satellite becomes confined to this halo core, there is no apparent overall shell expansion anymore, indicating that stripping has stopped, as expected. The inner satellite shells show slow gradual contraction, e.g., the mean density within the inner 10% shell has increased by $\sim 50\%$ compared to the initial configuration. This is consistent with the prediction based on adiabatic invariants, where the internal frequencies ω are expected to increase by a factor of $\sqrt{2}$ due to the doubling of the restoring force, $\omega^2 \propto \bar{\rho} + \bar{\sigma}$.

It is important to note that the halo radius r where $\alpha = 1$ is more than three times larger than the radius ℓ of the satellite's 20% shell, indicating that the cease of stripping occurs significantly before the center of the bound satellite remnant coincides with the halo center.

In the circular merger case, to a good approximation, the satellite position r is a monotonically decreasing function of time, and so is $\alpha(r)$, as shown at the top and marked along the time axis of Fig. 5. The stripping moment of each shell is marked by the onset of a steep rise in the corresponding curve. Proceeding from the outside shells inwards, the stripping point of each shell can be identified with a specific halo radius r and a corresponding α , moving down monotonically from $\alpha \sim 3$ to flatter slopes. However, as the stripping point passes beyond the radius where $\alpha \sim 1$ (after ~ 380 Myr), when the satellite is left with less

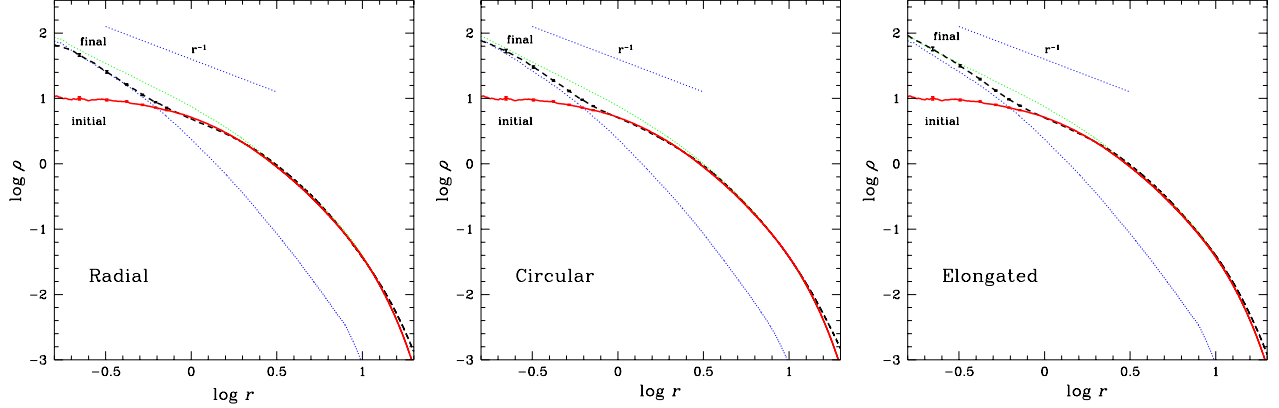


Fig. 6.— Halo density profile before (solid) and after (dashed) the merger with a compact satellite. Left: The radial merger simulation. A significant fraction of the satellite enters the halo core and settles at the halo center without depositing mass near $\alpha \sim 1$, which steepens the core into a cusp. Center: The circular merger. The lack of mass deposit near $\alpha \lesssim 1$ is apparent, resulting in steepening similar to the radial case. Right: The elongated merger. The steepening at $\alpha \lesssim 1$ is similar to the other cases. The error bars refer to Poisson errors in the r bins, and they are roughly spaced by the bin size. The thin dotted curves mark for reference the initial satellite profile (lower) and a straightforward sum of the initial profiles of halo and satellite (upper).

than $\sim 30\%$ of its original mass, the stripping slows down and eventually stops. The 20% and inner shells are never really stripped, and may even contract adiabatically, while the satellite's orbit continues to decay very slowly towards the halo center. The fact that even in this case of circular orbit the stripping seems to practically stop near $\alpha \sim 1$, not far from the behavior in the radial-orbit case, indicates that the estimate of tidal radius based on the Jacoby integral may indeed be an underestimate.

Fig. 6 shows the density profile of the halo before and after the mergers. For the standard, compact satellite, either on radial or circular orbit, the figure demonstrates the inevitable steepening of the profile in the core region, as expected. In the case of radial merger, the slight depletion of final density in the region near $\alpha \sim 1$, compared to the slight increment in halo density at larger radii, is consistent with no mass transfer in this region while the orbit of the remaining satellite continues to decay into smaller radii. A similar effect is also seen in the circular case, though it is somewhat weaker, as expected. Not surprisingly, the steepening seen at $\alpha \lesssim 1$ in the elongated merger case is not very different from the steepening seen in the two other cases.

Fig. 7 refers to similar mergers, but with the initial central satellite density scaled down

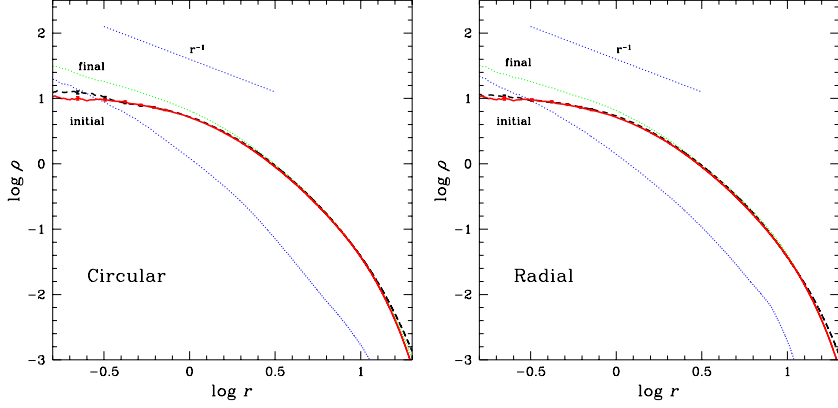


Fig. 7.— Halo density profile before (solid) and after (dashed) the merger with a puffy satellite, whose density has been scaled down by a factor of 3.3 compared to the compact satellite. Left: the radial merger simulation. Right: the circular merger simulation. Notation is as in Fig. 6. The puffy satellite loses most of its mass in the outer halo, leaving the halo core practically unaffected.

by a factor of ~ 3.3 (with $\ell_s = 2.5$ and $\sigma_s = 61.4$ compared to $\ell_s = 1$ and $\sigma_s = 18.7$ in the compact case). In this case, almost all the satellite mass is stripped before the satellite orbit decays to the $\alpha \leq 1$ zone, and as a result the halo core is practically unaffected.

Our general expectations based on the crude analytic estimates are thus confirmed by the single-merger simulations. The NFW inner slope of $\alpha = 1$ is a robust lower bound; a flatter density core cannot survive as long as bound satellites bring enough mass into the inner halo and thus deposit it near the halo center. This provides a simple and robust explanation for why the cusp slopes seen in cosmological N-body simulations of CDM models are typically $\alpha > 1$. It implies that the only way to enable a flatter core is by suppressing the settling of satellites in the core. The simulations demonstrate that puffy satellites are indeed disrupted outside the core and leave the core structure undamaged. Possible scenarios for how to achieve this will be discussed in §8.

7. CONVERGENCE TO AN ASYMPTOTIC CUSP

The tidal mass transfer in halo regions where the slope is $\alpha > 1$ and the actual convergence to an asymptotic cusp are analyzed in an associated paper (Dekel *et al.* 2002). We provide a preview of this analysis here for the completeness of the discussion.

We develop a simple prescription for tidal mass transfer by relating every shell ℓ in

the initial satellite with a “deposit” radius r in the halo. This is done by equating the encompassed mass within ℓ in the initial satellite with the stripped satellite mass in the halo inside r after the merger, $m(\ell) = m_{\text{fin}}(r)$. This correspondence can be expressed in terms of α :

$$\frac{\bar{\rho}(r)}{\bar{\sigma}(\ell)} = \psi[\alpha(r)], \quad (15)$$

where $\bar{\rho}(r)$ and $\bar{\sigma}(\ell)$ are as before the initial mean density profiles of the halo and the satellite. What makes this prescription useful is that $\psi(\alpha)$ is found to be quite insensitive to the specific nature of the merger (see below). Several authors (e.g., Syer & White 1998; Klypin 1999a) applied the crude resonance condition $\psi = 1$. However, the α dependence of the tidal force, and in particular its vanishing at low α , imply that $\psi(\alpha)$ should be a monotonically *decreasing* function of α . When we adopt the approximation of peeling layers off a fixed onion as above, we obtain from eq. (12) and eq. (11) that $\psi \propto (\alpha - 1)^{-1}$ and $\propto \alpha^{-1}$ respectively. When we also take into account the deposit at apocenter due to stripping at pericenter and the stretching and distortion of the inner satellite mass before it is being torn away³, we expect ψ to be smaller than unity even near $\alpha \sim 1$ and to decline further with α at $\alpha > 1$.

We then measure $\ell(r)$ and obtain $\psi(\alpha)$ in several different merger simulations like the ones described above. The measured $\psi(\alpha)$ is found to be qualitatively similar for the different merger cases, despite the very different orbits and initial density contrasts between satellite and halo. [This similarity can be seen from the resemblance of the final profiles $r(\ell)$ in Fig. 5]. An approximate empirical fit is obtained, for example, by $\psi(\alpha) = 0.5/\alpha$, with a spread of less than ± 0.1 about it in the different cases studied. The robustness of $\psi(\alpha)$ indicates that eq. (15) can serve as a useful approximate recipe for tidal mass transfer in the general case. We conclude that the simplified resonance condition, $\psi = 1$, does not provide a good approximation for where the satellite mass ends up. The actual mass transfer is more efficient ($\psi < 0.5$), and its relative efficiency gets higher in steeper regions of the halo profile.

If the mass transfer is described by eq. (15) with $\psi(\alpha)$ declining rapidly enough, we show in Dekel *et al.* (2002) that the profile evolves slowly towards an asymptotic stable power law with $\alpha_a \gtrsim 1$. We assume that the halo and satellite are drawn from a cosmological distribution (as predicted theoretically and seen in simulations); they are homologous, with their characteristic radii and densities scaling like $\ell_s/r_s \propto m^{(1+\nu)/3}$ and $\sigma_s/\rho_s \propto m^{-\nu}$, where $\nu \simeq 0.33$ for Λ CDM. Fig. 8 helps understanding intuitively the origin of an asymptotic slope due to the decreasing nature of $\psi(\alpha)$. We write $\bar{\rho}_{\text{final}}(r) = \bar{\rho}(r) + \bar{\sigma}(\ell)\ell^3/r^3$, and obtain for

³a decrease in satellite density before stripping has been seen in simulations (e.g. Klypin *et al.* 1999a, Fig. 6; Hayashi *et al.* 2002)

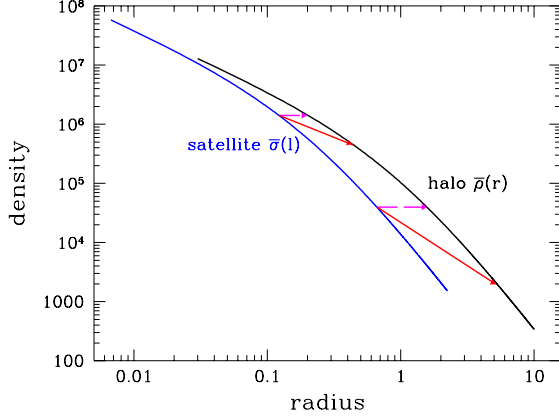


Fig. 8.— A schematic illustration of satellite mass deposit in the halo. Shown are an NFW halo profile $\bar{\rho}(r)$, and a homologous satellite $\bar{\sigma}(\ell)$ properly shifted to the left and upwards. The arrows connect shell radii ℓ to the halo radii where they are deposited r . The horizontal dashed arrows refer to stripping when stretching is ignored, $\psi(\alpha) = 1$. This would steepen the profile, as steep regions of $\bar{\sigma}(\ell)$ are deposited at flatter regions of $\bar{\rho}(r)$. The solid arrows illustrate realistic stripping after stretching. The vertical displacements, which grow with r , refer to $\psi(\alpha) < 1$. The slope at ℓ may be flatter than the slope at r such that the mass tends to be deposited at larger r and the result is flattening of the halo profile.

the change of the local slope in a merger

$$\Delta\alpha(r) \propto -\frac{d}{dr} \left(\frac{\bar{\sigma}(\ell) \ell^3}{\bar{\rho}(r) r^3} \right). \quad (16)$$

While every power law is a self-similar solution, $\Delta\alpha(r) = 0$, it is not necessarily a stable one. For example, with $\psi = \text{const.}$ one would have obtained $\Delta\alpha(r) > 0$ everywhere (because ℓ/r is decreasing with r), namely a continuous steepening towards $\alpha = 3$. On the other hand, a realistic mass transfer where ψ is decreasing with r may produce a stable fixed point where $\Delta\alpha = 0$ and the second derivative is negative. A rigorous linear perturbation analysis determines the rate of convergence and yields an equation for the value of the asymptotic slope α_a under a sequence of mergers with the same mass ratio m/M :

$$\Delta\alpha \propto \alpha(\alpha - 3)\psi'(\alpha)/\psi(\alpha) + 3 \ln[(m/M)^{-\nu}\psi(\alpha)] = 0.$$

The solutions for m/M large enough are typically in the range $1 < \alpha_a \leq 1.5$. For a sequence of mergers with a cosmological distribution of mass ratios we obtain an asymptotic slope comparable to the solution of eq. (7) with $m/M \simeq 0.3$.

In order to test the linear analysis, we perform toy simulations of the profile buildup by cosmological mergers, where we implement the mass-transfer recipe, eq. (15), with $\psi(\alpha) = 0.5/\alpha$. Fig. 9 shows the convergence of α at a fixed r to the asymptotic value. The profile

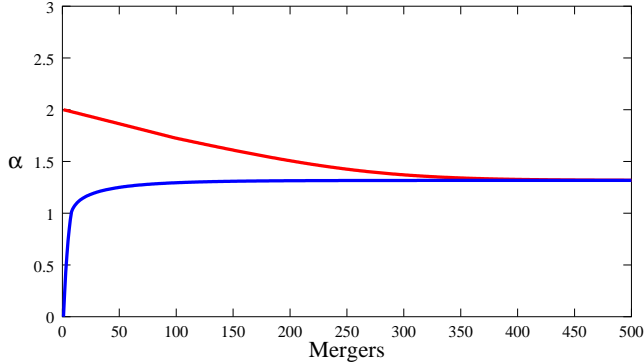


Fig. 9.— Toy-simulation evolution of slope α at $r = 0.1r_s$ due to a sequence of mergers with mass ratio $m/M = 0.3$. The initial profile is eq. (1) with α_0 either zero or 2. When $\alpha < 1$, the slope steepens rapidly to $\alpha > 1$ within a few mergers and then it converges slowly from either side towards an asymptotic value.

actually evolves through momentary profiles which are more relevant for comparison with real halos at different times during their buildup process; they resemble in shape the generalized NFW profile, with an inner cusp growing slowly from $\alpha = 1$ to $\alpha = \alpha_a$. We find a weak sensitivity to the cosmological power spectrum of perturbations.

8. A FLAT CORE BY STIMULATED FEEDBACK?

Our robust result is that a cusp of $\alpha > 1$ develops in dark-matter halos whenever mergers bring enough bound clumps to reside in the inner parts of halos. It implies that a way to maintain a flat core is by preventing bound clumps from settling in the core. This can be achieved if the cores of satellite halos were puffed up significantly by processes other than the gravity of dark matter, such that they are practically disrupted while apocenter is still in the outer halo. Stellar feedback effects, which seem not to be strong enough for straightforwardly turning a cusp into a core in a final large halo (Geyer & Burkert 2001; Gnedin & Zhao 2002), are possibly sufficient for the necessary indirect puffing-up of the merging satellites.

Gnedin & Zhao (2002) estimate that direct feedback effects may reduce the central halo densities by a factor of 2 to 6. Based on our simulations with puffed-up satellites (Fig. 7), this may be enough by itself to avoid the steepening from a core to a cusp in the framework of the merging scenario. The strength of the effect depends on how deep in the potential well the gaseous disk resides before it is blown away, which is determined by the baryonic spin. The possibility that baryons in the merging satellites have lost angular momentum due to over-cooling before regaining it by feedback (Navarro & Steinmetz 2000 and references

therein; Maller & Dekel 2002) allows one to consider lower spin values than measured in today’s disk galaxies, and thus obtain stronger effects on the dark matter.

In fact, one can think of special circumstances within the hierarchical buildup scenario that may boost up the feedback effects even further and help maintaining flat cores. We sketch here such a scenario, based on enhanced feedback in merging satellites due to the tidal compression of the baryons.

Consider a satellite made of dark-matter and a typical fraction of baryons merging with the halo on a typical eccentric orbit, which takes the satellite through the halo core to an apocenter in the outer halo a few times before it decays to inside the core region (as in our radial and elongated merger simulations). Assume that cooling in the satellite is efficient such that before the satellite passes through the halo core the baryons are already concentrated in the satellite core, making, say, a half-and-half mixture with the dark matter there. In every passage of the satellite through the halo core, where $\alpha < 1$, the tides compress the satellite into high densities (Fig. 5), creating shocks and stimulating an efficient burst of star formation. (The tides may also induce accretion of material including massive stars from the core of the host galaxy onto the satellite). By the time the satellite is turning around in the following apocenter outside the halo core, the massive stars have produced supernova-driven winds which drive much of the gas out of the satellite. The satellite have already lost much of its outer dark-matter envelope at this point and is basically made of the original satellite core plus most of the satellite baryons. If the satellite core loses half its bound mass in this gas blow-out, and the gas expulsion is instantaneous, then the satellite becomes completely unbound. But even if the expulsion is slow, the adiabatic invariants imply a density drop by a factor of ~ 8 . Thus, the remaining satellite is now much more susceptible to tidal stripping, which could disrupt it completely before it manages to settle in the halo core.

This scenario should be investigated in detail before one can consider it viable. At this point it is just an intriguing speculative proposal for enhanced feedback effects, based on the wisdom gained so far regarding the tidal effects, and very crude common wisdom regarding star formation and feedback (e.g. Dekel & Silk 1986).

9. DISCUSSION

The main result of this paper is that tidal compression enforces an inner cusp of slope $\alpha > 1$ in dark-matter halos which are subject to tandem mergers as in the Λ CDM cosmology. This robust effect explains the halo inner structure as seen in cosmological N-body simulations, and helps providing a tool for addressing other processes which may explain

the observed flat core in some galaxies. More details of the cusp formation are provided in an associated paper (Dekel *et al.* 2002) where we derive a simple prescription for tidal mass transfer and use it to show that successive cosmological mergers slowly lead to a stable asymptotic cusp slightly steeper than $\rho \propto r^{-1}$.

Syer & White (1998) (and independently Nusser & Sheth 1999) also addressed the profile resulting from mergers and obtained somewhat different results, which one should try to understand. They implemented the simplified model of tidal stripping at resonance, $\psi = 1$, ignoring the α dependence (e.g., the compression at $\alpha < 1$ and the gradual stretching at $\alpha > 1$). According to their algorithm, the steepening or flattening of the profile is determined solely by whether the satellite inner density is higher or lower than that of the halo. This prescription allows a long-term survival of a core of $\alpha < 1$ and it introduces an explicit dependence on the power spectrum of fluctuations — both in conflict with the findings in cosmological simulations. For each of several different power spectra they followed a sequence of mergers and saw an apparent convergence to a different self-similar profile. When we substitute the recipe $\psi = 1$ in eq. (16), we find that $\Delta\alpha$ is always positive, for any merger and at any r . Indeed, when trying to repeat the Syer & White toy simulations with higher resolution and following more mergers we actually find that the profile does not really converge to a stable cusp but rather continue to steepen slowly towards $\alpha_0 = 3$. Only when using the revised stripping prescription where ψ is decreasing with α do we obtain convergence to a flatter asymptotic profile. The asymptotic profile obtained via the revised stripping model is more robust to the cosmological model. In particular, the effect of tidal compression drives the profile to $\alpha \gtrsim 1$ independent of the fluctuation power spectrum, and the cosmological dependence of the ultimate asymptotic slope is weakened by the fact that the profile is determined by mergers of relatively large mass ratio.

Somewhat puzzling is the finding of power-spectrum dependence in the profile resulting from a sequence of N-body mergers by Syer & White, and especially the apparent slope flatter than $\alpha = 1$ found in one of their cases. It is puzzling because these simulations should have automatically included the correct tidal effects. We can only suspect that the main shortcomings of their N-body simulations are the limited resolution within the cusp region (only 8000 particles in the whole halo) and perhaps the fixed narrow range of satellite masses.

The gravitational processes leading to a cusp are modeled in our analysis as tidal effects during the buildup of the halo by a sequence of mergers. This picture is likely to be valid in the CDM hierarchical clustering scenario, where numerous sub-galactic halos exist on all scales and are continuously merging (Klypin *et al.* 1999b; Moore *et al.* 1999a; Springel *et al.* 2001). However, a cusp, though somewhat flatter, is reported to be seen also in simulations

where the initial fluctuations had less power on small scales, thus suppressing the number of sub-galactic satellites and the associated merger rate (Moore *et al.* 1999b; Bullock, Kravtsov & Colin 2001). Since we find that the asymptotic cusp formed in CDM is driven by mergers with relatively massive satellites (Dekel *et al.* 2002), and since such mergers do happen even when small-scale power is suppressed, it is possible that the cusp is driven by mergers in this case as well. If a cusp also forms when the merger picture is not strictly valid, it would imply that the gravitational processes involved in the halo buildup somehow mimic a behavior similar to the merger case. We note in particular that the tidal compression in the core is expected to amplify density perturbations and possibly make them behave in certain ways like merging satellites. More generally speaking, the halo buildup is a complex gravitational process that can probably be modeled in more than one way. The merger picture is only one possible toy model, within which the origin of the cusp is understood in simple terms.⁴

Our result implies a *necessary* condition for the survival of cores in halos — that satellites should be prevented from adding mass to the halo cores. This could be avoided in a CDM scenario if feedback processes puff up the satellites and make them disrupt before they merge with the halo cores. We have not explicitly addressed in this paper the *sufficient* conditions for the formation of cores, but one can imagine that a sequence of mergers with low-density satellites, where the mass is predominantly deposited outside the inner region, would indeed flatten the inner regions. Other processes may also contribute to the development of halo cores, such as the angular-momentum losses of a big temporary rotating bar (Weinberg & Katz 2002), or the delicate resonant reaction of halo-core orbits to the tidal perturbation by the satellite, which could be a strong effect if the dark-matter distribution is much smoother than the current state-of-the-art N-body simulations (Katz & Weinberg 2002). Nevertheless, our analysis implies that such cores would survive only if they are not perturbed by significant mass transfer from merging satellites.

The cusp/core problem is only one of the difficulties facing galaxy formation theory within the CDM cosmology. It turns out that other main problems can also be modeled by tidal effects in mergers, and may also be resolved by the inevitable feedback processes. For example, in Maller & Dekel (2002) we address the angular-momentum catastrophe, where simulations including gas produce disks significantly smaller than the galactic disks observed (Navarro & Steinmetz 2000 and references therein), and with a different internal distribution of angular momentum (Bullock *et al.* 2001; van den Bosch, Burkert & Swaters 2001). We

⁴We encounter a similar duality, for example, when one manages to explain the origin of galactic spin alternatively via tidal torque theory applied to shells and by summing up the orbital angular momenta in a cosmological sequence of mergers (Maller, Dekel & Somerville 2001).

first construct a toy model for the angular-momentum buildup by mergers based on tidal stripping and dynamical friction, which helps us understand the origin of the spin problem as a result of over-cooling in satellites. We then incorporate a simple model of feedback, motivated by Dekel & Silk (1986), and find that it can remedy the discrepancies, and in particular explain the low baryon fraction and angular-momentum profiles in dwarf disk galaxies. Feedback effects may also provide the cure to the missing dwarf problem, where the predicted number of dwarf halos in CDM is much larger than the observed number of dwarf galaxies (Klypin *et al.* 1999b; Moore *et al.* 1999a; Springel *et al.* 2001; Bullock, Kravtsov & Weinberg 2000). The successes of such toy models in matching several independent observations indicate that they indeed capture the relevant basic elements of the complex processes involved, and in particular that feedback effects may indeed provide the cure to the main problems of galaxy formation in CDM. The alternative solution involving Warm Dark Matter (e.g., Hogan & Dalcanton 2000; Bode, Ostriker & Turok 2001) seems to still suffer to some extent from the cusp/core problem, it may still fail to reproduce the angular-momentum profile in galaxies, and it may be an overkill where the formation of dwarf galaxies is totally suppressed once the inevitable feedback effects are included (Bullock 2001). The speculative alternatives involving self-interacting dark matter (Spergel & Steinhardt 2000) are even more problematic.

Acknowledgments

We acknowledge stimulating discussions with Itai Arad, George Blumenthal, Andi Burkert, Doug Lin and Gary Mamon. This research has been supported by the US-Israel Bi-National Science Foundation grant 98-00217, the German-Israel Science Foundation grant I-629-62.14/1999, and NASA ATP grant NAG5-8218.

REFERENCES

Barnes, J.E. & Hernquist, L. 1991, ApJL, 370, L65.
Binney, J. & Tremaine, S. 1987, Galactic Dynamics (Princeton University Press), BT
Bode, P., Ostriker, J.P. & Turok, N. 2001 (astro-ph/0010389)
Borriello, A. & Salucci, P. 2001, MNRAS, 323, 285
van den Bosch, F.C., Burkert, A. & Swaters, R.A. 2001, MNRAS, 326, 1205
van den Bosch, F.C., Robertson, B.E., Dalcanton, J.J. & de Blok, W.J.G. 2000, AJ, 119,

Bullock, J.S. 2001, astro-ph/0111005

Bullock, J.S. Dekel, A., Kolatt, T.S., Kravtsov, A.V., Klypin, A.A., Porciani, C. & Primack, J.R. 2001, ApJ, 555, 240

Bullock, J.S., Kravtsov A.V. & Colin P. 2001, ApJL, in press

Bullock J.S., Kravtsov A.V. & Weinberg D.H. 2000, ApJ, 539, 517

Cole, S. & Lacey, C. 1996, MNRAS, 281, 716

de Blok, W.J.G., McGaugh, S.S., Bosma, A. & Rubin, V.C. 2001, ApJL, 552, L23

Dekel, A., Arad, I., Ben David, O. & Birnboim, Y. 2002, submitted

Dekel, A. & Maller, A.H. 2002, in The Mass of Galaxies at Low and High Redshift, eds. R. Bender & A. Renzini (Springer-Verlag, ESO Astrophysics Symposia)

Dekel A. & Silk J. 1986, ApJ, 303, 39

Geyer, M.P. & Burkert, A. 2001, MNRAS, 323, 988

Ghigna, S., Moore, B., Governato, F., Lake, G., Quinn, T. & Stadel, J. 1998, MNRAS, 300, 146

Ghigna, S., Moore, B., Governato, F., Lake, G., Quinn, T. & Stadel, J. 2000, ApJ, 544, 616

Gnedin, O.Y. & Zhao, H. 2002, MNRAS (astro-ph/0108108)

Hayashi, E., Navarro, J.F., Taylor, J.E., Stadel, J. & Quinn, T. 2002, astro-ph/0203004

Hogan C.J. & Dalcanton J.J. 2000, PRD, 62

Katz, N. & Weinberg, M.D. 2002, in Cozumel

Klypin, A., Gottlber, S., Kravtsov, A.V. & Khokhlov, A.M. 1999a, ApJ, 516, 530

Klypin, A.A., Kravtsov, A.V., Bullock, J.S. & Primack, J.R. 2001, ApJ, 554, 903

Klypin, A., Kravtsov, A.V., Valenzuela, O. & Prada, F. 1999b, ApJ, 522, 82

Lokas, E.L. & Hoffman, Y. 2000, ApJL, 542, L139

Maller A.H. & Dekel A. 2002, MNRAS, submitted

Maller A.H., Dekel A. & Somerville, R.S. 2001, MNRAS, in press (astro-ph/0105168)

Mihos, J.C. & Hernquist, L. 1996, ApJ, 464, 641

Moore, B., Ghinga, S., Governato, F., Lake, G., Quinn, T., Stadel, J. & Tozzi, P. 1999a, ApJL, 524, L19

Moore, B., Governato, F., Quinn, T., Stadel, J. & Lake, G. 1998, ApJL, 499, L5

Moore, B., Quinn, T., Governato, F., Stadel, J. & Lake, G. 1999b, MNRAS, 310, 1147

Navarro J.F., Eke, V.R. & Frenk C.S. 1996, MNRAS, 283, L72

Navarro J.F., Frenk C.S. & White S.D.M. 1995, MNRAS, 275, 56

Navarro J.F., Frenk C.S. & White S.D.M. 1996, ApJ, 462, 563

Navarro J.F., Frenk C.S. & White S.D.M. 1997, ApJ, 490, 493

Navarro J.F. & Steinmetz M. 2000, ApJ, 538, 477

Nusser, A. & Sheth, R. 1999, MNRAS, 303, 685

Pearce, F.R., Thomas, P.A. & Couchman, H.M.P. 1993, MNRAS, 286, 865

Power, C., Navarro, J.F., Jenkins, A., Frenk, C.S., White, S.D.M., Springel, V., Stadel, J & Quinn, T. 2002, MNRAS, submitted (astro-ph/0201544)

Salucci, P. 2001, MNRAS, 320, L1

Salucci, P. & Burkert, A. 2000, ApJL, 537, L9

Spergel, D.N. & Steinhardt, P.J. 2000, PRL, 84, 3760

Springel, V., White, S.D.M., Tormen, G. & Kauffmann, G. 2001, MNRAS, 328, 726

Syer, D. & White, S.D.M. 1998, MNRAS, 293, 337

Weinberg, M.D. & Katz, N. 2002, astro-ph/0110632